

# Enantioselectivity of Protoporphyrinogen Oxidase-Inhibiting Herbicides

Ujjana B. Nandihalli,<sup>a</sup> Mary V. Duke,<sup>a</sup> John W. Ashmore,<sup>b</sup> Vincent A. Musco,<sup>b</sup> Robert D. Clark,<sup>c</sup> and Stephen O. Duke,<sup>a\*</sup>

<sup>a</sup> Southern Weed Science Laboratory, Agricultural Research Service, United States Department of Agriculture, PO Box 350, Stoneville, Mississippi 38776, USA

<sup>b</sup> Rohm and Haas Company, 727 Norristown Road, Spring House, Pennsylvania 19477, USA

<sup>c</sup> Monsanto Company, 800 North Lindbergh Avenue, St. Louis, Missouri 63167, USA

(Revised manuscript received 5 August 1993; accepted 17 November 1993)

**Abstract:** Protoporphyrinogen oxidase (Protox) was inhibited stereoselectively by three pairs of enantiomers belonging to diphenyl ether (DPE) and pyrazole phenyl ether (PPE) herbicide classes. The (*R*) enantiomers were 10- to 44-fold more active than the (*S*) enantiomers as inhibitors of Protox from barley etioplasts. Similarly, the (*R*) enantiomers caused green barley tissue to accumulate greater amounts of porphyrins and caused greater tissue damage than the (*S*) enantiomers. The (*R*) enantiomers competed more successfully with [<sup>14</sup>C]acifluorfen than the (*S*) enantiomers for the binding sites on Protox. In the PPE class, the in-vitro and in-vivo activity differences were wider in the isopropyl pairs than in the *n*-propyl pairs. The DPE enantiomers were tested on ten dicotyledonous and six monocotyledonous weed species and ten crops for weed control and crop safety. In general, neither enantiomer had pre-emergence activity on monocotyledons, but the (*R*) enantiomer provided some monocotyledonous weed control when applied post-emergence. On dicotyledons, the (*R*) enantiomer provided excellent pre-emergence control, whereas the (*S*) enantiomer was inactive. The (*R*) enantiomer caused no injury to corn, cotton, peanuts, rice, sorghum, or soybeans applied pre-emergence, but it severely injured crops when applied post-emergence. There was a positive correlation between the activities of the compounds at the molecular, cellular and whole plant levels. The only molecular property differences found to account for differences in activity between members of chiral pairs were steric parameters.

## 1 INTRODUCTION

Bicyclic compounds of several chemical classes cause rapid peroxidative damage to plants by causing rapid accumulation of the photodynamic porphyrin pathway intermediate, protoporphyrin IX (Proto IX).<sup>1–3</sup> The molecular site of action of these herbicides is plastid protoporphyrinogen oxidase (Protox).<sup>3–6</sup> Inhibition of Protox causes accumulation of protoporphyrinogen IX (Protoporphyrin IX) which leaves the plastid<sup>7</sup> and is apparently oxidized rapidly outside the plastid to form Proto IX in

extraplastidic membranes.<sup>8,9</sup> In the presence of light and molecular oxygen, Proto IX generates singlet oxygen, a highly reactive oxygen species responsible for membrane lipid peroxidation.

These compounds are competitive inhibitors of Protox that apparently compete for the Protox IX binding site.<sup>10–13</sup> They mimic one half of the Protox IX molecule.<sup>3,13,14</sup> Furthermore, these compounds apparently compete for the same binding site.<sup>10,12,13</sup> Structure–activity studies of various chemical classes of these compounds have been conducted,<sup>13–17</sup> with different results, depending on the class and the type of activity measured.

Chirality can be an important structural determinant in herbicidal activity, and this information has potential in elucidating the nature of herbicide binding sites.

\* To whom correspondence should be addressed.

† Mention of a trademark or product does not constitute an endorsement of the product by the US Department of Agriculture and does not imply its approval to the exclusion of other products that may also be suitable.

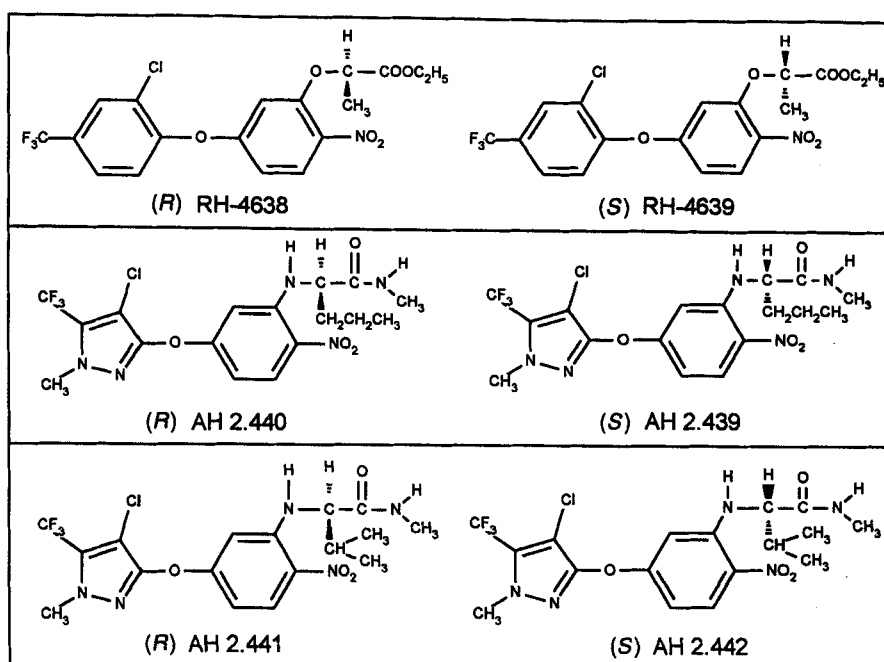


Fig. 1. Structures of chiral compounds used in this study.

The (*R*) enantiomers of the aryloxyphenoxy herbicides which inhibit acetyl CoA carboxylase are significantly more active than the (*S*) enantiomers.<sup>18,19</sup> The (*R*) enantiomers of certain triazines are more active than the (*S*) in causing certain growth effects,<sup>20,21</sup> whereas the (*S*) enantiomers of the same compounds are required for good inhibition of photosystem II.<sup>22</sup> The topic of chiral discrimination at the  $Q_B$  binding site is discussed by Bowyer *et al.*<sup>23</sup> Chirality in the *meta*-substitution of the *para*-nitrophenyl ring of Protox-inhibiting herbicides has been reported previously to affect activity at the molecular and whole plant levels.<sup>14,24,25</sup> In each of these previous studies, only one chiral pair was studied and little or no analysis of the molecular property differences was made.

In this paper we compare the activities of three enantiomeric pairs of Protox inhibitors (Fig. 1) (one diphenyl ether and two pyrazole phenyl ethers) at the molecular, tissue, and whole plant levels. Activity at each level was consistent with activity at the other levels, indicating that the enantiomeric effect is due to differential activity at the molecular level. Furthermore, the only molecular parameters apparently responsible for the differences in activity between members of chiral pairs were the steric differences.

## 2 MATERIALS AND METHODS

### 2.1 Synthesis of Protox inhibitors

#### 2.1.1 Pyrazole phenyl ethers

3-Amino acid-substituted pyrazole nitrophenyl ethers are readily prepared by aromatic nucleophilic substitution

of the fluoro precursor (Fig. 2). Purification exploits the hydrophilicity of the product salts and their insolubility in acid. Conversion to amides is accomplished by a carbonic mixed anhydride. This scheme avoids racemization at the  $\alpha$ -carbon, which was monitored by the NMR shifts induced by (*R*)-2,2,2-trifluoro-1-(9-anthryl)ethanol (Aldrich Chemical Co.†) in deuteriochloroform.<sup>26</sup> Analytical NMR spectra were obtained at 300 or 360 MHz on an IBM AF-300 or on a Bruker AM-360 spectrometer, respectively. Measurements of  $^1\text{H}$ - $^1\text{H}$  nuclear Overhauser enhancement (NOE) were taken at 300 MHz with a Varian XL-300 spectrometer. Elemental analyses were carried out by Atlantic Microlab, Inc., of Norcross, GA. Melting points are uncorrected.

Syntheses of the *N*-aryl amino acid analogs (AH 2.440 and AH 2.439) were begun by combining fluoronitrophenyl pyrazole<sup>27</sup> (6 mmol) with potassium carbonate (13 mmol) and a slight excess of amino acid (6.5 mmol) in 30 ml *N*-methylpyrrolidinone. The reaction flask was then purged with nitrogen and heated to 65°C following addition of a catalytic amount of anhydrous copper(II)-fluoride (0.5 mmol). After 20 h, the mixture was poured into 100 g litre<sup>-1</sup> sodium chloride/0.1 M sodium hydroxide (600 ml) and residual fluoronitrophenyl pyrazole ether extracted into cyclohexane + diethyl ether (2 + 1 by volume: 300 ml). *N*-Aryl amino acid product was precipitated from the aqueous subphase by addition of 10% hydrochloric acid (100 ml) and extracted into ethyl acetate (200 ml). The organic phase was washed three times with 10% sodium chloride and dried over magnesium sulfate; evaporation of solvent under vacuum gave the *N*-aryl amino acid-substituted pyrazole phenyl ethers in 77–95% yield.

To produce *N*-aryl-*N'*-methyl amino amides, the

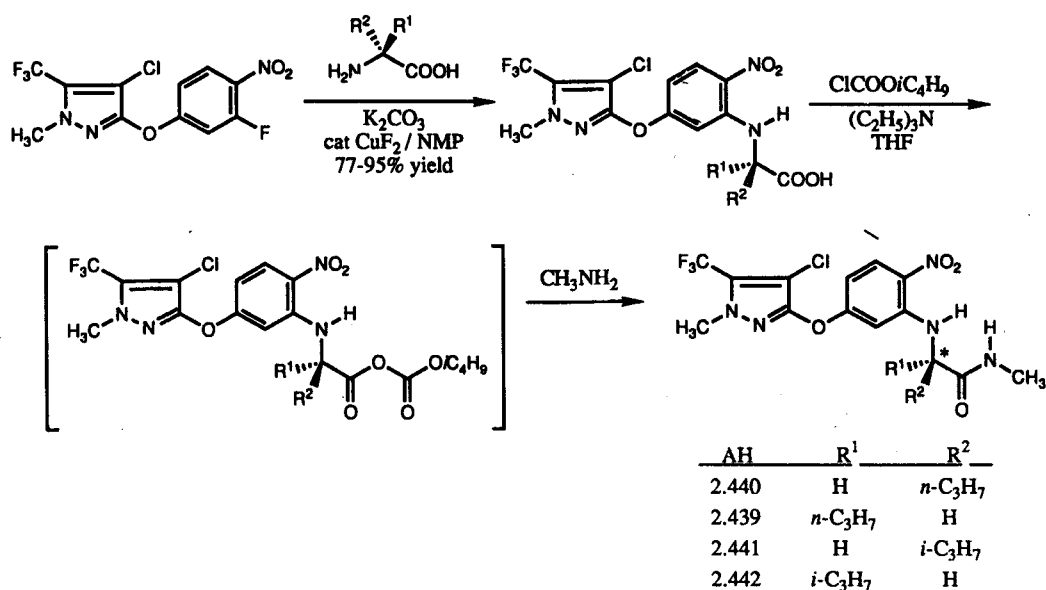
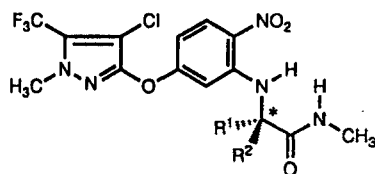
Fig. 2. Scheme for synthesis of *N*-pyrazoloxypheyl amino acids.

TABLE 1  
Physical Properties of Pyrazole Phenyl Ether Enantiomers



AH	[ <sup>1</sup> H]NMR deuteriochloroform, δ, multiplicity <sup>a</sup> (area <sup>b</sup> )	*	<i>m.p.</i> (°C)	[α] <sub>D</sub> <sup>25</sup>	anal(C, H, Cl, N)
2.440	0.98 tr (3 H), 1.50 m (2 H), 1.83 m <sup>b</sup> , 2.01 m, 2.80 d (3 H), 3.81 dtr, 3.98 q (3 H), 6.26 q, 6.42 d, 6.50 dd, 8.23 d, 8.27 d	R	161.5–163	–75.7	45.54, 4.32, 7.74, 15.35
2.439			S	161.5–162.5	+77.4
2.441	1.07 d (3 H), 1.09 d (3 H), 2.47 m, 2.82 d (3H), 3.72 tr, 2.442 2.47 m, 2.82 d (3 H), 3.72 tr, 3.98 q (3 H), 6.28 q, 6.44 d, 6.48 dd, 8.23 d, 8.41 d	R	194–195	–71.2	45.66, 4.34, 7.78, 15.36
2.442			S	195.5–196.5	+61.3
			calcd (C <sub>17</sub> H <sub>19</sub> ClN <sub>5</sub> F <sub>3</sub> O <sub>4</sub> )		45.39, 4.26, 7.88, 15.57

<sup>a</sup> d, doublet; tr, triplet; q, quartet; dd, doublet of doublets; dtr, doublet of triplets; m, multiplet.

<sup>b</sup> Resonances integrate to an area corresponding to 1H unless otherwise indicated.

appropriate aryl amino acid (4.6 mmol) was taken up in anhydrous tetrahydrofuran (30 ml) with triethylamine (0.8 ml; 5.2 mol) in a dry flask and chilled under nitrogen by immersion in dry ice/acetone. *iso*-Butyl chloroformate (5 mmol) was diluted with tetrahydrofuran (10 ml) and added dropwise so as to maintain the flask temperature at or below –20°C; residual reagent was rinsed in from the addition funnel with 5 ml additional solvent and the reaction flask transferred to an ice water bath. After 30 min at 0°C, 40% methylamine (18 mmol) diluted to 10 ml in tetrahydrofuran was added rapidly to the turbid reaction mixture. The mixture was kept at 0°C for 20 min, then allowed to warm to ambient temperature. Dilution into water gave the product as a yellow precipitate which was collected and washed sequentially with sodium

hydroxide (0.1 M), water, hydrochloric acid (0.1 M) and again with water. Oven drying under vacuum gave amino amides in 74–80% yield. The physical properties of these compounds are given in Table 1.

The amide *N*-methyl doublet resonances from side-chain substituents and, unexpectedly, the pyrazole *N*-methyl singlet were all shifted upfield to varying degrees ( $\Delta\delta$  –0.025 to –0.055 ppm) by anthryl ethanol complexation for both enantiomers. All *N*-methyl resonances exhibited greater shifts for the (*R*) than for the (*S*) enantiomers ( $\Delta\Delta\delta$  0.004 to 0.009 ppm). In contrast, the spectral lines arising from alkyl protons were uniformly shifted more for the (*S*) enantiomers, especially for the terminal methyl groups ( $\Delta\Delta\delta$  –0.008 to –0.022 ppm). In the most striking case, the differential intramolecular

chiral shift by (*R*) anthryl reagent nearly collapses the underlying inequivalence of the  $\beta$ -methyl groups in AH 2:442 to a  $\Delta\delta$  of 0.004 ppm; the corresponding separations for AH 2:442 (or AH 2:441) alone and/or complexed AH 2:441 are 0.014 and 0.015 ppm, respectively. Aromatic [ $^1\text{H}$ ]NMR signals showed no detectable differential shift.

The optical purities of the enantiomer preparations were found to be at least 90%.

### 2.1.2 Diphenyl ethers

RH-4639 (Fig. 1) preparation was begun with a stirred solution of ethyl (*S*)-lactate (34.4 g; 300 mmol) in dry pyridine (200 ml) that was cooled to below 10°C and *p*-toluenesulfonyl chloride (77.0 g; 405 mmol) was added portionwise. The mixture was stirred until it became homogeneous, stoppered, and stored overnight in a freezer. The mixture was poured on to c. 1 litre of crushed ice and the product separated as an oil. After the ice had melted, the mixture was extracted with diethyl ether. The ether extract was washed twice with cold hydrochloric acid (6 M) and three times with water, and dried over sodium sulfate and potassium carbonate. Removal of the solvent left a yellow oil (81 g) which was dissolved in hexane (3 litre) at room temperature. The hexane solution was cooled to -70°C and the fine white needles that crystallized were collected to yield 71 g (87%) of ethyl (*S*)-2-(*p*-toluenesulfonyloxy) propionate, mp < 37°C.

A mixture of potassium 5-(2-chloro-4-trifluoromethylphenoxy)-2-nitrophenoxide (11.4 g; 30.7 mmol) and ethyl (*S*)-2-(*p*-toluenesulfonyloxy)propionate (6.0 g; 22.1 mmol) in dry acetonitrile (40 ml) was heated and refluxed until all the tosylate had been consumed. The acetonitrile was removed by rotary evaporation. The residue was triturated with ether and the ether solution was filtered through a plug of neutral alumina. The alumina plug was washed with fresh ether and the eluate was concentrated to yield 7.2 g (75%) of ethyl (*R*)-(-)-2-(5-(2-chloro-4-trifluoromethylphenoxy)-2-nitrophenoxy)propionate (Fig. 1, RH-4638) as a pale yellow oil. [ $^1\text{H}$ ]NMR (deuteriochloroform)  $\delta$  1.23 (3H, t,  $J = 7.3$ ), 1.69 (3H, d,  $J = 6.9$ ), 4.19 (2H, m), 4.77 (1H, q,  $J = 6.9$ ), 6.54 (2H, m), 7.20 (1H, d,  $J = 8.4$ ), 7.59 (1H, dd,  $J = 8.6, 1.8$ ), 7.79 (1H, d,  $J = 1.8$ ), 7.93 (1H, d,  $J = 9.2$ ). IR (deuteriochloroform) 1750, 1615, 1595, 1325, 1140  $\text{cm}^{-1}$ .  $[\alpha]_{\text{D}}^{25} = -37.75^\circ$ .

The ethyl (*R*)-2-(*p*-toluenesulfonyloxy)propionate was prepared from ethyl (*R*)-lactate in 85% yield using the procedure described above for the (*S*) isomer. The tosylate was reacted with potassium 5-(2-chloro-4-trifluoromethylphenoxy)-2-nitrophenoxide, following the same procedure as above to generate ethyl (*S*)-(+)-2-(5-(2-chloro-4-trifluoromethylphenoxy)-2-nitrophenoxy)propionate (RH 4639, Fig. 1) as a pale yellow oil in 52% yield. Its [ $^1\text{H}$ ]NMR and IR spectra were identical to those of the (*R*) enantiomer.  $[\alpha]_{\text{D}}^{25} = +32.37^\circ$ .

## 2.2 Plant material

For Prottox assays and tissue bioassays, barley (*Hordeum vulgare* L. cv. Morex) was grown in flats in a commercial greenhouse substrate ('Jiffy Mix'; JPA, West Chicago, IL) and watered with distilled water. Etiolated barley plants were grown in the dark at 25°C for six days and green barley plants were grown at 25°C under continuous white light of 500  $\mu\text{mol m}^{-2} \text{s}^{-1}$  photosynthetically active radiation (PAR) and >90% relative humidity for eight days.

For greenhouse assays of pyrazole phenyl ether herbicidal activity, cucumber (*Cucumis sativus* L. cv. Straight Eight) and barley (cv. Morex) were grown in 10  $\times$  10 cm pots in silt loam soil. Greenhouses were maintained at 30°C on a 14-h day with supplemental lighting, and watering was by subirrigation.

For greenhouse assays of the diphenyl ether chiral pair, seeds of different species were planted in trays measuring 20  $\times$  25  $\times$  10 cm or 25  $\times$  35  $\times$  10 cm (width  $\times$  length  $\times$  height) for pre-emergence tests and in 10-cm diameter pots for post-emergence tests. The soil was locally obtained (Spring House, PA) silty loam top soil with 1.0–1.5% organic matter amended with sand in a two-to-one (silty loam to sand) mix. Seeds were sown 1.25 cm deep. The trays were placed in greenhouses in which temperatures ranged from 22 to 35°C with 16-h photoperiods maintained with artificial light providing 400–500  $\mu\text{mol m}^{-2} \text{s}^{-1}$  at bench level at night.

## 2.3 Prottox assay

Etioplast Prottox preparations were made from six-day-old, dark-grown barley leaves as before.<sup>15</sup> Prior to assay, protein content of plastid preparations was determined by the method of Bradford<sup>28</sup> with bovine serum albumin as a standard. Extracts were diluted to 4 mg protein  $\text{ml}^{-1}$  in resuspension buffer.

Protogen IX was prepared according to Jacobs and Jacobs<sup>29</sup> with the following modifications. Proto IX stock solution (0.5 mM) was reduced to Protogen IX using approximately one-eighth volume of freshly ground sodium amalgam. The resulting colorless solution was adjusted to pH 7.5 by addition of an equal volume of five-fold strength assay buffer, consisting of 2-[4-(2-hydroxyethyl)piperazin-1-yl]ethanesulfonic acid (HEPES 500 mM; pH 7.5) and ethylenediaminetetra (acetic acid) (EDTA, 25 mM). Residual amalgam and porphyrin aggregates were removed by passing the solution through a 0.22- $\mu\text{m}$  nylon syringe-tip filter. Dithiothreitol (DTT) was added to the Protogen IX solution to a final concentration of 2 mM. For the Prottox assay, the plastid extracts were pre-incubated with herbicides for at least 15 min on ice. The herbicides were dissolved in ethanol and the control treatments contained equivalent amounts of ethanol. The assay mixture consisted of HEPES (100 mM; pH 7.5), EDTA, (5 mM),

DTT (2 mM) and about 2  $\mu\text{M}$  Protogen IX. The reaction was initiated by addition of 0.1 ml of plastid extract treated with the herbicide to 0.9 ml of assay mixture and monitored for 2 min at 30°C.

Fluorescence was monitored directly from the assay using a Shimadzu RF-5000U, temperature-controlled, recording spectrofluorometer with excitation and emission wavelengths set at 395 and 622 nm, respectively. Other workers have used excitation wavelengths between 400 and 409 nm and emission wavelengths between 632 and 636 nm for determining Proto IX, depending on the type of reaction medium used. In our reaction medium, the excitation and emission maxima for Proto IX were 395 and 622 nm, respectively. Formation of Proto IX was constant over the 2-min period. Auto-oxidation of Protogen IX to Proto IX in the presence of heat-inactivated (80°C) Protox could not be detected during the 2-min assay period.

## 2.4 Porphyrin determinations

All extractions for HPLC were made under a dim, green light source. Samples (0.22 g of barley leaf sections) were homogenized and extracted as before.<sup>15</sup> Determinations of Proto IX, Mg-Proto IX, Mg-Proto IX monomethyl ester, and protochlorophyllide (PChlide) were made as before by HPLC with spectrofluorometric detection.<sup>30</sup> All porphyrin compound levels are expressed on a molar basis per gram of fresh weight. All treatments for porphyrin samples were triplicated.

## 2.5 Herbicidal activities

### 2.5.1 Electrolyte leakage

In tissue section experiments, tissues were treated with the herbicides as before<sup>15,31</sup> by cutting 5-mm barley leaf sections (approximately 0.22 g) with a razor blade, and then placing them in a 6-cm-diameter polystyrene Petri dish in 5 ml of sucrose (10 g litre<sup>-1</sup>), 2-[*N*-morpholino]-ethanesulfonic acid (MES; 1 mM, pH 6.5) medium with or without herbicide dissolved in absolute ethanol. The discs were then incubated at 25°C in darkness for 20 h before exposure to 500  $\mu\text{mol cm}^{-2} \text{ s}^{-1}$  PAR for up to 24 h. Cellular damage was measured by detection of electrolyte leakage into the bathing medium with a conductivity meter as before.<sup>31</sup> Because of differences in background conductivity of different treatment solutions, results are expressed as changes in conductivity upon exposure to light. Previous studies have shown that Protox-inhibiting herbicides have no significant effect on cellular leakage in darkness. All treatments were triplicated.

### 2.5.2 Greenhouse studies

Pyrazole phenyl ether enantiomers were tested for post-emergence activity. Eleven-day-old cucumber and barley plants were thinned to six seedlings per pot and

herbicide treatments applied as solutions in acetone + water (90 + 10 by volume; 3.2 ml) supplemented with 'Latron' AG-98® (Rohm and Haas Co.) to 1.5 g litre<sup>-1</sup>. Serial dilution produced five rates for each compound and alternate rates were tested in duplicate. Three days after treatment, each species was evaluated for injury to aerial tissues; ratings ranged from 100 % for complete mortality to 0 % for plants virtually indistinguishable from control plants treated with the formulation blank. Injury was also evaluated by independent blind ranking, with controls included, from least (1) to most (36) injured by direct intercomparison. Such direct ranking is a somewhat higher resolution approach which can reduce distortions in variability at extreme ratings (i.e., 0 and 100 %).

The diphenyl ether chiral pair was tested for both pre-emergence and post-emergence activities in several crop and weed species, using a spray volume of 234 litre ha<sup>-1</sup>. The herbicides were dissolved in acetone before mixing with water. All applications were made with a continuous belt sprayer in which the test plants move mechanically under a fixed spray nozzle. After spray application, the pots were placed in a vented cabinet until dry and then placed in the greenhouse. The pre-emergence tests were watered overhead and the post-emergence tests were watered by subirrigation. Plants 14 to 21 days old (from planting) were sprayed in post-emergence treatments. Grasses were in the two- to four-leaf stage and dicotyledons were in the one- to two-true-leaf stage at this age. Observations were made two to three weeks after treatment using a 0 (no effect) to 100 % (complete mortality) rating system. The percent injury values are composites which include chlorosis, necrosis, inhibition of growth, and tip burning with the untreated control for comparison.

## 2.6 Binding studies

Barley etioplasts were isolated from etiolated barley seedlings as described previously.<sup>32</sup> The procedure of Tischer and Strotmann<sup>33</sup> was used to determine binding of [<sup>14</sup>C]acifluorfen to barley etioplasts in the presence or absence of enantiomers. Using previously reported methods,<sup>14</sup> etioplast membranes were mixed with [<sup>14</sup>C]-acifluorfen and centrifuged to pellet the membranes. The tubes were drained and the inner tube walls were wiped dry with cotton swabs (to remove any adhering [<sup>14</sup>C]-acifluorfen) without disturbing the pellets. A 100  $\mu\text{l}$  aliquot of tissue solubilizer ('Protosol'® New England Nuclear, Boston, MA) was added to pellets and heated in a water bath at 50°C for 15 min. The slurry was transferred to vials, and 12 ml of scintillation fluid ('Ecolume'®, ICN Biomedicals, Inc., Irvine, CA) was added for radioactivity measurements. The amount of [<sup>14</sup>C]acifluorfen bound was calculated from the radioactivity in the pellets.

## 2.7 Estimation of partition coefficients

Reversed-phase high-performance liquid chromatography (RP-HPLC) was used for the determination of octanol/water partition coefficients ( $P$ ) of herbicides.<sup>34,35</sup> The RP-HPLC technique involved determination of capacity factors ( $k'$ ) for a set of standard compounds with a wide range of known experimental partition coefficients. The  $k'$  values were calculated from the equation:

$$k' = (t_r - t_0)/t_0$$

where,  $t_r$  is the retention time of the compound and  $t_0$  is the retention time of the non-sorbed standard compound (acetone). A standard curve of  $\log P$  versus  $\log k'$  was constructed. Using the same HPLC conditions as in the standard curve, the capacity factors for the herbicides were determined. The  $\log P$  of herbicides was calculated using the linear regression equations of the form  $\log P = a + b(\log k')$ .

The HPLC system was composed of Water Associates components which included Model 510 pumps; a Model 712 autosampler; a Maxima 820 controller, and a Model 990 diode-array spectrophotometric detector. The column was a 250 × 4.6 mm (i.d.) Spherisorb 5 μm ODS-1, C-18 reversed-phase column. The mobile phase was methanol + water (75 + 25, by volume). A flow rate of 1.4 ml min<sup>-1</sup> was used and a column temperature of 28°C was maintained with a Waters Temperature Control and Column Heater Module. The injection volume was 5 μl. The herbicides and standard compounds were dissolved in methanol at 1 mg ml<sup>-1</sup> concentration. The detector was set at 254 nm. Three replicate determinations were made for each compound.

## 2.8 Molecular properties

The molecular properties of enantiomers were calculated using the computer software and procedures as described in our previous work.<sup>13,14</sup> Three-dimensional chemical structures were built from standard atoms and fragments stored in the library file of Chem-X software (Chemical Design Limited, Oxford, England). The structures were optimized by a semi-empirical molecular orbital program, MOPAC (Quantum Chemistry Program Exchange, No. 560, Dept. Chemistry, Indiana University, Bloomington, IN, USA; Version 6.0) using AM1 (Austin Model) hamiltonian.

## 3 RESULTS

### 3.1 Herbicidal properties

#### 3.1.1 Tissue bioassay

The (*R*) enantiomers of both Protox inhibitor families were significantly more effective than the (*S*) enantiomers in causing electrolyte leakage from barley leaf tissue (Fig.

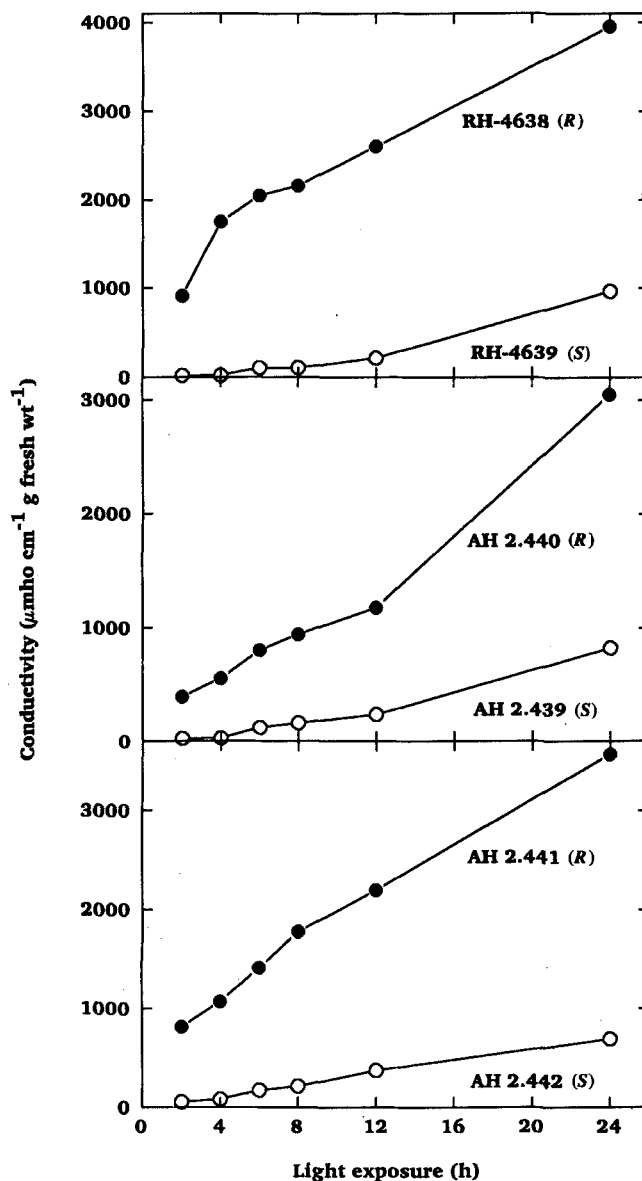


Fig. 3. Effects of compounds of Fig. 1 on electrolyte leakage from barley leaf sections exposed to 0.1 mM of each compound for 20 h in darkness and then exposed to 500 μmol m<sup>-2</sup> s<sup>-1</sup> PAR at time zero.

3). The differences in activity were obvious within 2 h of exposure to light for all chiral pairs. In the pyrazole phenyl ethers, the differences between (*R*) and (*S*) activity was greater for the isopropyl than the *n*-propyl pair.

#### 3.1.2 Greenhouse studies

In whole-plant studies in the greenhouse, (*R*) enantiomers of both Protox inhibitor families were significantly more herbicidal than the (*S*) enantiomers (Table 2, Fig. 4). In the case of the diphenyl ether chiral pair, the herbicidal activity was tested on a wide array of both monocotyledonous and dicotyledonous weed and crop species under both pre- and post-emergence regimes (Table 2). The (*R*) enantiomer was consistently more active than the (*S*) under all circumstances in all species. In general,

**TABLE 2**  
Pre- and Post-emergence Whole-Plant Activity of RH-4638 and RH-4639 on Monocotyledonous and Dicotyledonous Weeds and Crops

Species	Herbicide	Application rate ( $g\ ha^{-1}$ )					
		Pre-emergence			Post-emergence		
		38	75	150	20	38	75
<b>Monocotyledons</b>		-(injury rating)-					
<i>Zea mays</i> L.	RH-4638	0	0	30	— <sup>a</sup>	30	70
maize	RH-4639	0	0	0	—	0	0
<i>Oryza sativa</i> L.	RH-4638	0	0	0	—	40	75
rice	RH-4639	0	0	0	—	0	0
<i>Sorghum vulgare</i> L.	RH-4638	0	0	40	—	75	100
sorghum	RH-4639	0	0	0	—	0	0
<i>Triticum aestivum</i> L.	RH-4638	0	0	0	—	28	75
wheat	RH-4639	0	0	0	—	13	25
<i>Echinochloa crus-galli</i> (L.) Beauv.	RH-4638	0	0	23	43	53	75
barnyard grass	RH-4639	0	0	0	0	3	0
<i>Phalaris minor</i> Retz.	RH-4638	0	0	0	18	70	20
canary grass	RH-4639	0	0	0	0	0	0
<i>Setaria viridis</i> (L.) Beauv.	RH-4638	25	40	99	48	88	40
green foxtail	RH-4639	0	0	0	0	3	0
<i>Sorghum halepense</i> (L.) Pers.	RH-4638	0	0	0	28	80	85
johnsongrass	RH-4639	0	0	0	0	0	0
<i>Cyperus esculentus</i> L.	RH-4638	0	0	0	0	0	0
yellow nutsedge	RH-4639	0	0	0	0	0	0
<i>Brachiaria platyphylla</i> Nash	RH-4638	0	0	0	3	13	20
broadleaf signalgrass	RH-4639	0	0	0	5	3	0
<b>Dicotyledons</b>							
<i>Gossypium hirsutum</i> L.	RH-4638	0	0	0	—	100	100
cotton	RH-4639	0	0	0	—	35	99
<i>Arachis hypogaea</i> L.	RH-4638	0	0	0	—	30	20
peanut	RH-4639	0	0	—	—	0	0
<i>Brassica napus</i> L.	RH-4638	20	30	80	—	100	100
canola	RH-4639	0	0	30	—	25	99
<i>Beta vulgaris</i> L.	RH-4638	75	99	99	—	100	100
sugarbeet	RH-4639	0	0	95	—	20	15
<i>Helianthus annuus</i> L.	RH-4638	0	10	10	—	100	100
sunflower	RH-4639	0	0	0	—	40	50
<i>Glycine max</i> (L.) Merr	RH-4638	0	0	0	—	40	80
soybean	RH-4639	0	0	0	—	13	15
<i>Anoda cristata</i> (L.) Schlecht	RH-4638	0	25	78	100	90	100
anoda	RH-4639	0	0	0	5	5	0
<i>Convolvulus arvensis</i> L.	RH-4638	100	100	100	100	100	100
bindweed	RH-4639	0	0	0	10	10	25
<i>Xanthium strumarium</i> L.	RH-4638	0	25	20	100	100	100
cocklebur	RH-4639	0	0	0	10	5	0
<i>Euphorbia heterophylla</i> L.	RH-4638	0	100	100	100	98	95
wild poinsettia	RH-4639	0	0	0	5	8	90
<i>Tagetes</i> spp.	RH-4638	0	100	100	100	100	100
marigold	RH-4639	0	0	0	10	58	100
<i>Ipomoea lacunosa</i> L.	RH-4638	0	43	63	100	100	100
pitted morning glory	RH-4639	0	0	0	10	45	100
<i>Cassia obtusifolia</i> L.	RH-4638	0	10	50	58	83	100
sicklepod	RH-4639	0	0	0	0	0	0
<i>Sida spinosa</i> L.	RH-4638	—	—	—	93	93	95
prickly sida	RH-4639	—	—	—	0	48	80
<i>Abutilon theophrasti</i> (L.) Medic	RH-4638	20	70	100	100	100	100
velvetleaf	RH-4639	0	0	0	10	60	100
<i>Sinapis arvensis</i> L.	RH-4638	0	95	100	100	100	100
wild mustard	RH-4639	0	0	0	—	35	75

<sup>a</sup> No measurement made.

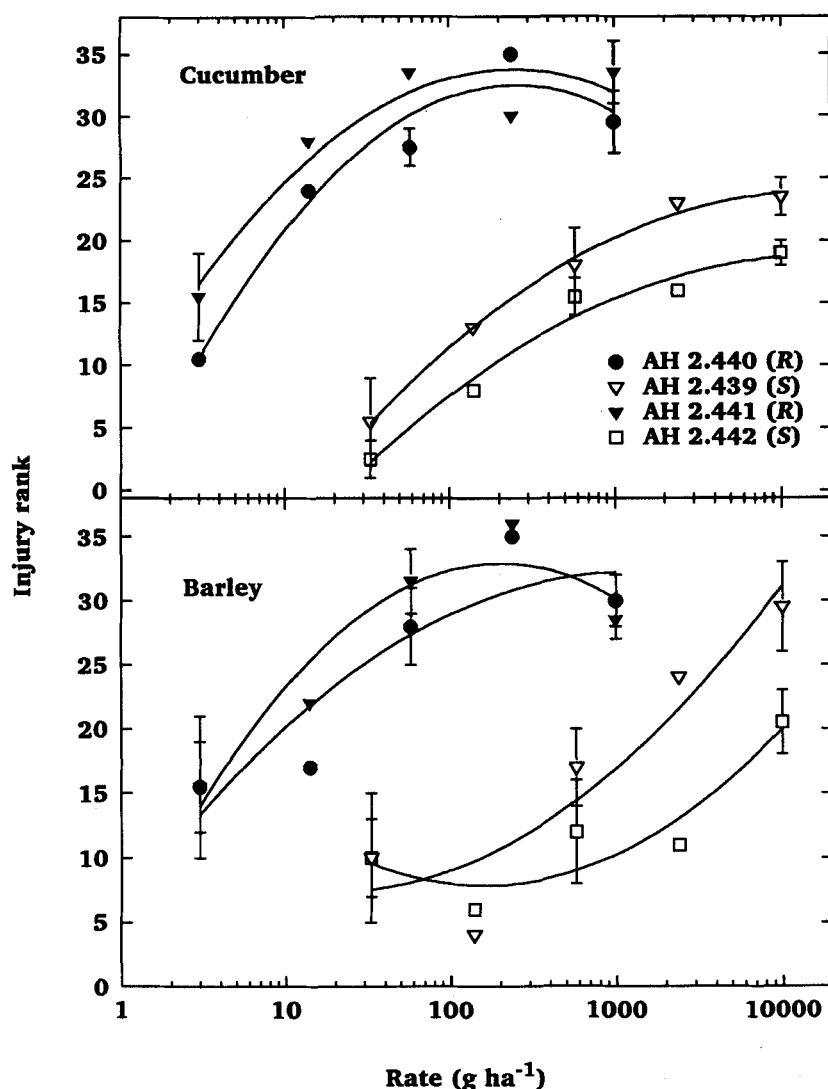


Fig. 4. Log dose response curves of herbicidal damage to intact cucumber and barley plants by the two chiral pairs of pyrazole phenyl ether herbicides.

both enantiomers had no pre-emergence activity on monocotyledons, but the (*R*) enantiomer provided some monocotyledon weed control when applied post-emergence. On dicotyledons, the (*R*) enantiomer provided excellent pre-emergence control, whereas the (*S*) enantiomer was inactive. The (*R*) enantiomer caused no injury to corn, cotton, peanuts, rice, sorghum, and soybeans applied pre-emergence, but caused severe injury to crops applied post-emergence.

The (*R*) enantiomers of the pyrazole phenyl ether chiral pairs were about 100-fold more active than their corresponding (*S*) enantiomers on both cucumber and barley in greenhouse studies (Fig. 4). The difference in activities between the (*R*) and (*S*) enantiomers of the isopropyl pair was slightly greater than that between the *n*-propyl pair. The shapes of the dose-response curves of the (*S*) enantiomers on barley were different from those of the (*R*) enantiomers or of either enantiomer on

cucumber. Other than this, the results were similar for both species.

### 3.2 Effects on the porphyrin pathway

The  $I_{50}$  values of the (*R*) members of all three chiral pairs were ten- to 44-fold smaller than those of the respective (*S*) enantiomers (Table 3, Fig. 5). Proto IX levels in (*R*) enantiomer-treated tissues were four- to 35-fold greater in (*R*) enantiomer-treated than in (*S*) enantiomer-treated tissues (Table 3). However, the levels of Proto IX in (*S*) enantiomer-treated tissues were 10- to 50-fold higher than that of the control. The largest differences were between the effects of AH 2.442 and AH 2.441, the isopropyl pair. This was due to AH 2.442 being the best Protox inhibitor and AH 2.441 being the weakest pyrazole phenyl ether Protox inhibitor. PChlide levels were increased slightly by the (*R*) enantiomers only. There were positive

**TABLE 3**  
Effects of Enantiomers on Protox Inhibition and Porphyrin Induction in Barley

Herbicides	Protox $I_{50}$ (nM)	Porphyrins	
		Proto IX (-nmoles g fresh wt <sup>-1</sup> )-	PChlide
Control		0.05	5.00
RH-4638 (R)	55	10.5	7.11
RH-4639 (S)	650	2.7	5.36
AH 2.440 (R)	30	11.4	7.44
AH 2.439 (S)	300	2.0	5.35
AH 2.441 (R)	12	14.8	8.54
AH 2.442 (S)	520	0.42	5.11

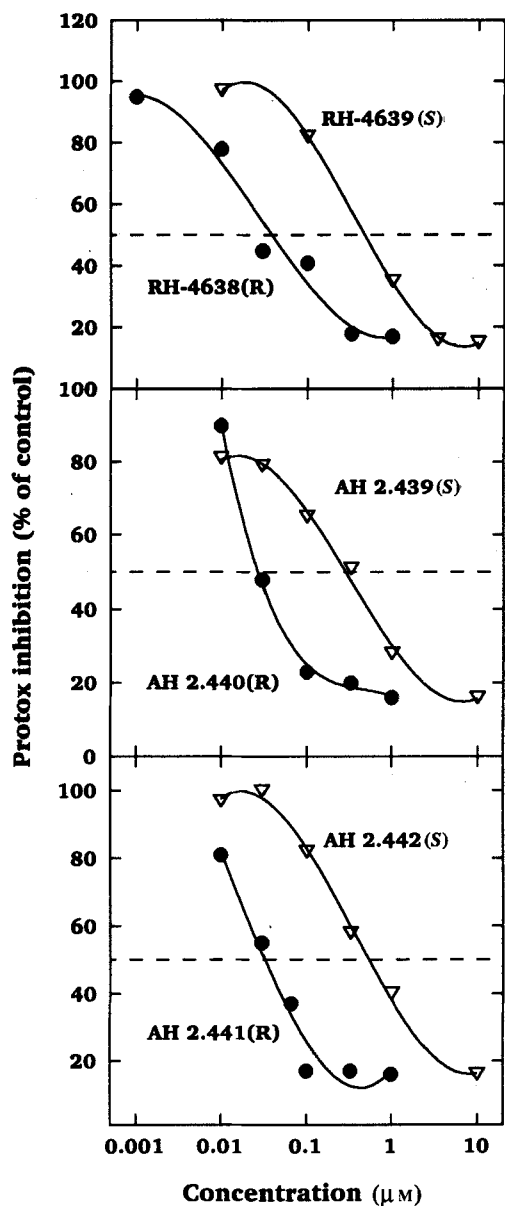


**Fig. 5.** Log dose response curves for inhibition of barley Protox with three chiral pairs of Protox inhibitors.

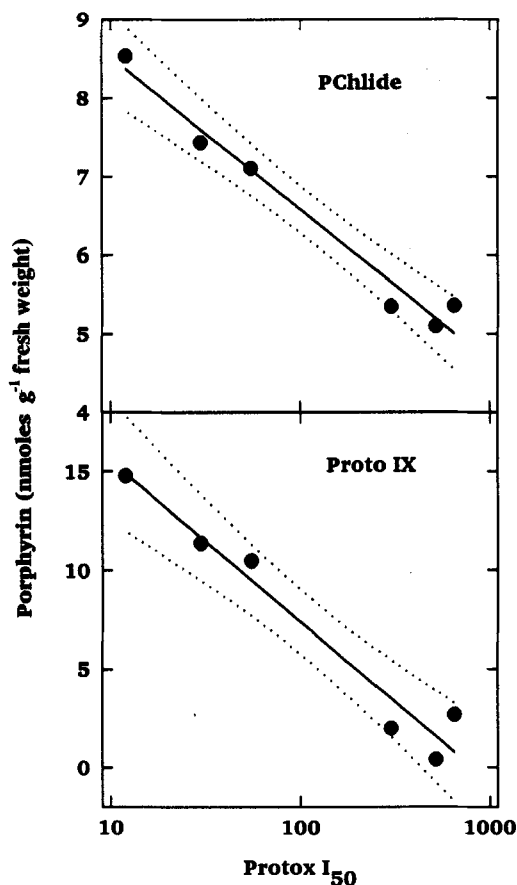


**Fig. 6.** Relationship between Protox  $I_{50}$  values and Proto IX, and PChlide accumulated in tissues treated with 100  $\mu\text{M}$  of each of the compounds of Fig. 1. The solid line is the first-order regression. The dotted lines are 95% confidence intervals. Regression coefficients for the regression between log Protox  $I_{50}$  and Proto IX, log Protox  $I_{50}$  and PChlide, and Proto IX and PChlide are 0.976, 0.986, and 0.993, respectively.

correlations between the effectiveness of the herbicides as Protox inhibitors, the amount of Proto IX accumulation, and the amount of PChlide accumulation (Fig. 6).

### 3.3 Binding properties and Log P

The log  $P$  values of each chiral pair were identical or very close to each other (Table 4). Competitive binding

**TABLE 4**  
Log  $P$  Values for Chiral Pairs Used in These Studies

Herbicide	Log $P$
RH-4638 (R)	4.54
RH-4639 (S)	4.53
AH 2.440 (R)	4.25
AH 2.439 (S)	4.25
AH 2.441 (R)	4.15
AH 2.442 (S)	4.14

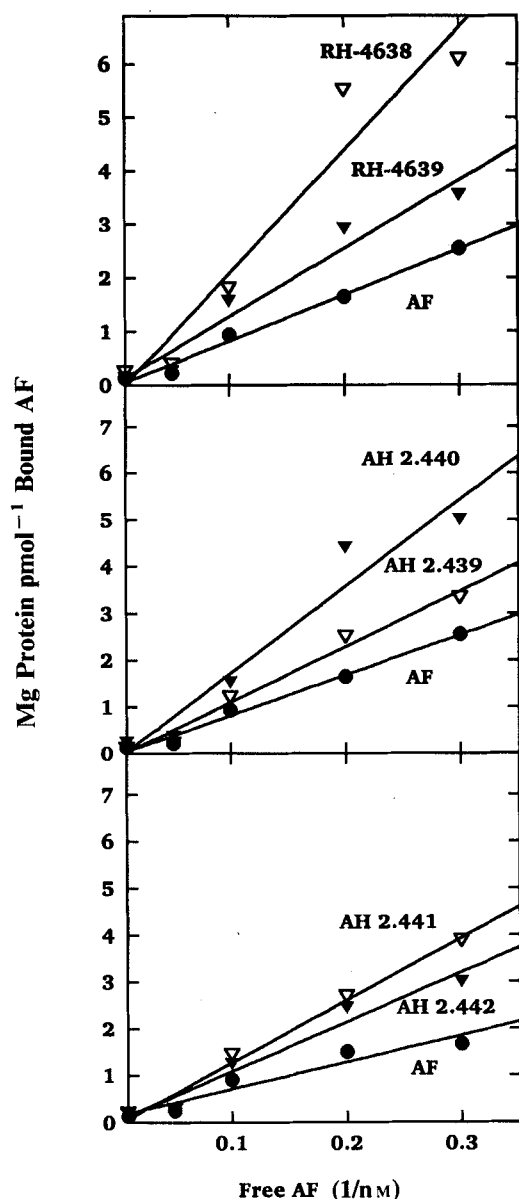


Fig. 7. Binding of [ $^{14}\text{C}$ ]acifluorfen (AF) in the presence of 100 nM of chiral pairs.

of chiral components with [ $^{14}\text{C}$ ]acifluorfen was strikingly different (Fig. 7). The (*R*) enantiomers competed better with acifluorfen than the (*S*) enantiomers for the active site(s) on Protox.

### 3.4 Molecular properties

Molecular modeling techniques were applied to examine whether the differential biological activities of enantiomers could be attributed to differences in their molecular properties. Figure 8 shows three-dimensional lowest energy conformers of chiral pairs as optimized by semi-empirical hamiltonian methods. From optimized structures it is apparent that the chiral pairs differ with respect to spatial arrangement mainly around the chiral centers.

The bulk (van der Waal's volume) and electronic properties were not significantly different except in their nucleophilic superdelocalisability and dipole moment (Table 5). The (*S*) enantiomers had larger dipole moments than the (*R*) enantiomers.

## 4 DISCUSSION

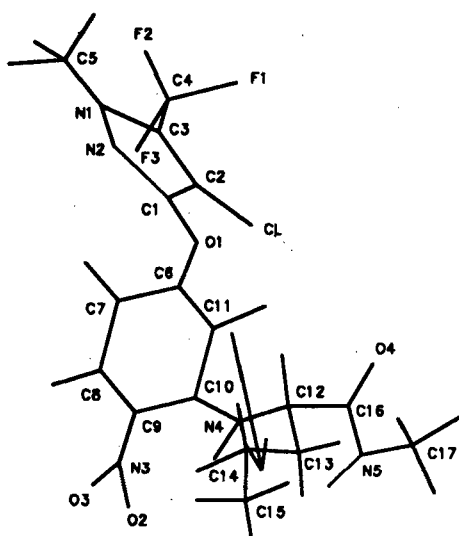
The (*R*) enantiomers of chiral pairs of both diphenyl ethers and pyrazole phenyl ethers in this study were markedly more active than their (*S*) counterparts. Because the chirality of all three pairs is centered around the first carbon of a *meta* ether or amino substitution of the nitrophenyl ring, the mechanistic explanation for chiral specificity is likely to be the same for all three chiral pairs.

Although  $\log P$  is an important determinant in activity of Protox inhibitors at the molecular level,<sup>13,14</sup> it was not influenced by chirality.  $\log P$  strongly influences transport ability of bioactive compounds across cellular barriers and their partitioning into membranes. Because of their similar  $\log P$  values, differential transport behavior was apparently not responsible for the observed differences in biological activity between chiral pairs.

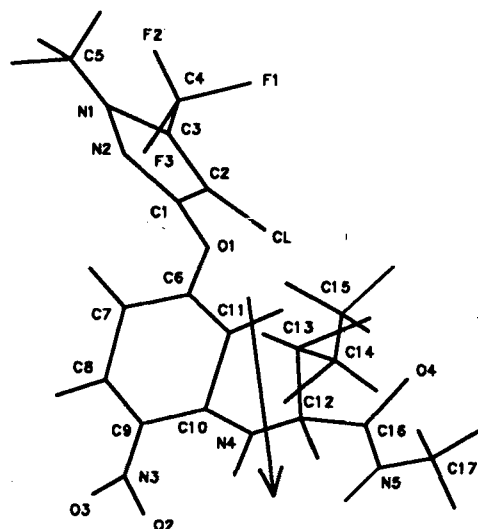
There was a negative correlation between the Protox  $\log I_{50}$  values and the amount of Proto IX accumulated (Fig. 6). Similar correlations have been found previously with pyrazole phenyl ethers and phenopylate analogues.<sup>15,30</sup> Although the range of PChlide levels was not great, there was also an inverse correlation between Protox  $\log I_{50}$  values and the amount of PChlide accumulated (Fig. 6). Increases in PChlide in Protox inhibitor-treated tissues may be due to reentry of cytoplasm-concentrated Proto IX into the plastid porphyrin pathway after large amounts of Proto IX have accumulated in the cytoplasm.<sup>36</sup>

The discriminating capacity of an enzyme for its substrate is based on a chemical relationship that involves complementarity with respect to the physicochemical characteristics of involved groups as well as their steric configurations. Apart from the character of the chiral center (carbon in the present case) as such, its location in the molecule is critical to its biological significance. If it is situated at the position which interacts with the active site, one could expect a high degree of stereospecificity. This would cause large differences in biological activity between enantiomers. Thus, one can conclude that the carbon chiral centers in DPE and pyrazole phenyl ethers that we have studied are probably located on the molecule at a position which interacts with or overlaps the active site of Protox.

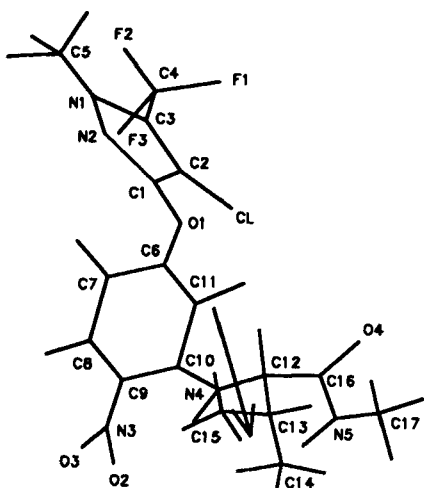
Binding studies in which Proto IX has been used to displace Protox-inhibiting herbicides competitively from the Protox molecule support the view that Protox inhibitors are competitive inhibitors.<sup>12</sup> The kinetics of inhibition are those of a competitive inhibitor with respect to the Proto IX substrate.<sup>11</sup> Furthermore,



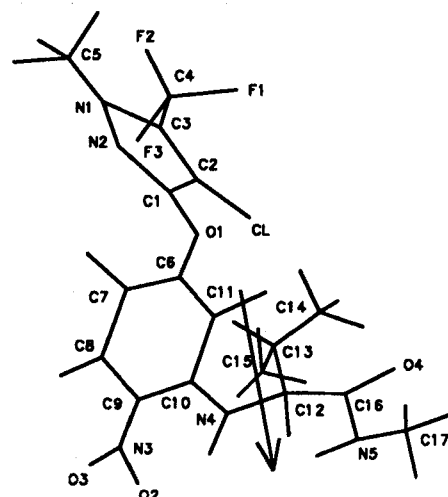
AH 2.440 (R)



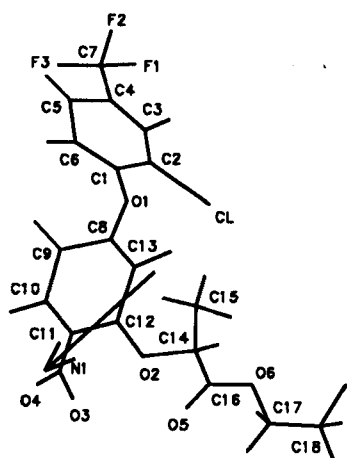
AH 2.439 (S)



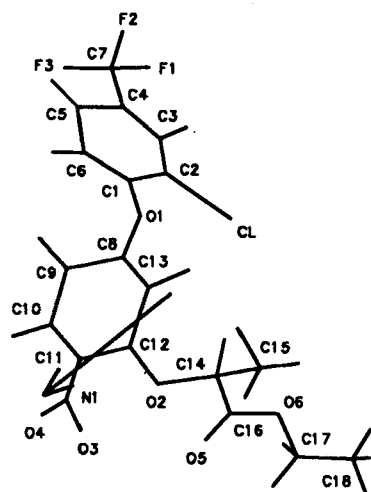
AH 2.441 (R)



AH 2.442 (S)



RH-4638 (R)



RH-4639 (S)

Fig. 8. Enantiomer structures optimized by MOPAC using AM1 hamiltonian. The *para*-nitrophenyl ring is oriented the same for each of the structures. Arrows in the structures represent the dipole moments.

TABLE 5  
Bulk and Electronic Molecular Properties of Chiral Compounds

Parameters <sup>a</sup>	-Enantiomer-					
	RH4638 (R)	RH4639 (S)	AH 2.440 (R)	AH 2.239 (S)	AH 2.441 (R)	AH 2.442 (S)
van der Waal's volume (Å <sup>3</sup> )	288.6	287.0	298.5	313.1	301.2	312.8
-MEP volume (Å <sup>3</sup> )	361.2	370.8	302.0	297.5	300.0	291.2
+MEP volume (Å <sup>3</sup> )	239.9	227.0	207.1	212.5	204.9	212.5
HOMO energy (eV)	-10.07	-10.07	-9.28	-9.28	-9.24	-9.24
LUMO energy (eV)	-1.21	-1.24	-0.97	-1.03	-1.05	-1.05
Superdelocalisability (eV)						
HOMO	-0.198	-0.199	-0.216	-0.217	0.216	-0.217
LUMO	-1.654	-1.609	-2.06	-1.95	-2.15	-1.91
Electrophilic	-8.67	-8.66	-9.27	-9.28	-9.26	-9.27
Nucleophilic	52.77	42.86	65.40	78.17	69.40	98.61
Dipole moment (D)	4.565	4.993	2.680	3.160	2.675	4.040

<sup>a</sup> MEP, molecular electrostatic potential; HOMO, highest occupied molecular orbital; LUMO, lowest unoccupied molecular orbital.

comparisons of the structures of Protogen IX and Protox inhibitors have shown that these compounds mimic one half of the Protogen IX molecule rather closely.<sup>3,13,35</sup> Thus, an allosteric effect of these inhibitors on substrate binding is unlikely.

The molecular properties of enantiomers calculated from semi-empirical methods were not significantly different (Table 5). Thus, the properties of these enantiomers do not differ significantly in isotropic environments, but differ only by their mirror-type, three-dimensional structures. It is then their mirror-type structures (i.e. the spatial arrangement of groups around the chiral center) which are critical for the closer fit required for efficient binding to Prototox. High biological activity in the effective isomers involves a tight fit to the active site with restricted steric freedom, and failure of the other isomer to give the same tight fit results in relatively low affinity. It was evident that the (S) isomers competed less effectively with AF for the Prototox binding site than the (R) isomers (Fig. 7). The basis of isomer discrimination appears to be related entirely to differences in the spatial orientation of methyl, *n*-propyl, and iso-propyl groups in the (R) and (S) isomers when they are bound to the Prototox active site.

#### ACKNOWLEDGEMENTS

The authors thank Drs Judy and Nick Jacobs for sharing a preprint of their recent paper. BASF Corp. generously provided [<sup>14</sup>C]acifluorfen.

#### REFERENCES

- Duke, S. O., Lydon, J., Becerril, J. M., Sherman, T. D., Lehnen, L. P. Jr. & Matsumoto, H., *Weed Sci.*, **39** (1991) 465-73.
- Duke, S. O., Becerril, J. M., Sherman, T. D., Lydon, J. & Matsumoto, H., *Pestic. Sci.*, **30** (1990) 367-78.
- Nandihalli, U. B. & Duke, S. O., *Amer. Chem. Soc. Symp. Ser.*, **524** (1993) 62-78.
- Matringe, M., Camadro, J.-M., Labbe, P. & Scalla, R., *FEBS Lett.*, **245** (1989) 35-8.
- Matringe, M., Camadro, J.-M., Labbe, P. & Scalla, R., *Biochem. J.*, **269** (1989) 231-5.
- Witkowski, D. A. & Halling, B. P., *Plant Physiol.*, **90** (1989) 1239-42.
- Jacobs, J. M. & Jacobs, N. J., *Plant Physiol.*, **101** (1993) 1181-8.
- Jacobs, J. M., Jacobs, N. J., Sherman, T. D. & Duke, S. O., *Plant Physiol.*, **97** (1991) 280-7.
- Lee, H. J., Duke, M. V. & Duke, S. O., *Plant Physiol.*, **102** (1993) 881-9.
- Varsano, R., Matringe, M., Magnin, N., Mornet, R. & Scalla, R., *FEBS Lett.*, **272** (1990) 369-75.
- Camadro, J.-M., Matringe, M., Scalla, R. & Labbe, P., *Biochem. J.*, **277** (1991) 17-21.
- Matringe, M., Mornet, R. & Scalla, R., *Eur. J. Biochem.*, **209** (1992) 861-8.
- Nandihalli, U. B., Duke, M. V. & Duke, S. O., *Pestic. Biochem. Physiol.*, **43** (1992) 193-211.
- Nandihalli, U. B., Duke, M. V. & Duke, S. O., *J. Agric. Food Chem.*, **40** (1992) 1993-2000.
- Nandihalli, U. B., Sherman, T. D., Duke, M. V., Fisher, J. D., Musco, V. A., Becerril, J. M. & Duke, S. O., *Pestic. Sci.*, **35** (1992) 227-35.
- Osabe, H., Morishima, Y., Goto, Y. & Fujita, T., *Pestic. Sci.*, **35** (1992) 187-200.
- Watanabe, H., Otori, Y., Sandmann, G., Wakabayashi, K. & Böger, P., *Pestic. Biochem. Physiol.*, **42** (1992) 99-109.
- Duke, S. O. & Kenyon, W. H., In *Herbicides—Chemistry, Degradation and Mode of Action, Vol. III*, ed. P. C. Kearney

- & D. D. Kaufmann. Marcel Dekker, New York, 1988, pp. 71–116.
19. Walker, K. A., Ridley, S. M. & Harwood, J. L., *Biochem. J.*, **254** (1988) 307–10.
  20. Omokawa, H., Takeuchi, M. & Konnai, M., *Pestic. Sci.*, **35** (1992) 87–90.
  21. Omokawa, H. & Konnai, M., *Pestic. Sci.*, **35** (1992) 83–6.
  22. Omokawa, H. & Konnai, M., *Agric. Biol. Chem.*, **54** (1990) 2373–8.
  23. Bowyer, J. R., Camilleri, P. & Vermaas, W. F. J., In *Topics in Photosynthesis—Vol. 10, Herbicides*, ed. N. R. Baker & M. P. Percival. Elsevier, Amsterdam, 1991, pp. 27–85.
  24. Camilleri, P., Gray, A., Weaver, K. & Bowyer, J. R., *J. Agric. Food Chem.*, **37** (1988) 519–23.
  25. Hallahan, B. J., Camilleri, P., Smith, A. & Bowyer, J. R., *Plant Physiol.*, **100** (1992) 1211–26.
  26. Pirkle, W. H. & Hoekstra, M. V., *J. Amer. Chem. Soc.*, **98** (1976) 1832–9.
  27. Moedritzer, K. & Rogers, M. D., *US Patent 4,964,895*, 1990.
  28. Bradford, M. M., *Anal. Chem.*, **72** (1976) 248–54.
  29. Jacobs, N. J. & Jacobs, J. M., *Enzyme*, **28** (1976) 206–29.
  30. Sherman, T. D., Duke, M. V., Clark, R. D., Sanders, E. F., Matsumoto, H. & Duke, S. O., *Pestic. Biochem. Physiol.*, **40** (1991) 236–45.
  31. Kenyon, W. H., Duke, S. O. & Vaughn, K. C., *Pestic. Biochem. Physiol.*, **24** (1985) 240–50.
  32. Sherman, T. D., Becerril, J. M., Matsumoto, H., Duke, M. V., Jacobs, N. J. & Duke, S. O., *Plant Physiol.*, **97** (1991) 280–7.
  33. Tischer, W. & Strotmann, H., *Biochim. Biophys. Acta*, **460** (1977) 113–25.
  34. Ellgehasen, H., D'Hondt, C. & Fuerer, R., *Pestic. Sci.*, **12** (1981) 219–27.
  35. Nandihalli, U. B., Duke, M. V. & Duke, S. O., *J. Agric. Food Chem.*, **40** (1993) 1993–2000.
  36. Lehnen, L. P. Jr, Sherman, T. D., Becerril, J. M. & Duke, S. O., *Pestic. Biochem. Physiol.*, **37** (1990) 239–48.